研究論文

Conceptual Design Description of a CT Fueler for JT-60U

RAMAN Roger* and ITAMI Kiyoshi
JT-60U Experimental Division, Naka Fusion Research Establishment,
Japan Atomic Energy Research Institute, Ibaraki 311-0193, Japan

(Received 21 January 2000 / Accepted 23 August 2000)

Abstract

This paper is a conceptual design description of a Compact Toroid (CT) fueling system for JT-60U. In the proposed system, the CT fueler injects 0.4 mg toroids of Deuterium fuel at up to 10 Hz into a 2 T, JT-60U discharge at a speed of 300 km/s. For discharges with a density of 3×10^{19} m^{-3}, this translates to about 6% fuel addition per pulse and a fueling rate of 2.3 Pa·m^3/s in the form of deep fueling. The fueling per pulse (as percent fueling) is about twenty times greater than that needed for a reactor of the ITER class as the projected fuelling rate for an ITER class reactor is 0.3% fuel addition per pulse (at 20 Hz operation). The total absolute fueling rate is about 10% of that needed for a similar reactor, as the projected CT mass fuelling rate for an ITER class reactor is about 44 mg/s. The CT length is about 20–30% of the JT-60U minor radius.

The 10 Hz power system will be composed of 100 accelerator modules and 80 formation bank modules each rated at 1.3 kJ. These will be powered by next generation capacitors and recent design spark gap switches. The CT injector will require magnetic shielding. Design description of a novel passive SuperConductor (SC) shield to meet this requirement is provided.

Keywords:
compact troid, multiple injection, fueling, tokamak, JT-60U, super conductor shield

1. Introduction

The current reference fueling schemes for reactors are based on gas puffing and pellet injection. These techniques are reasonably well demonstrated on present tokamaks. However, these fueling schemes cannot penetrate the plasma deeply in fusion reactors.

Perkins *et al.* [1,2] proposed injecting Compact Toroids (CTs) of dense DT plasma into tokamaks to achieve deep fueling and experiments have been conducted on smaller tokamaks. This CT injector consists of three regions – formation, compression, and acceleration. Fuel gas is puffed into the formation region, and a combination of magnetic field and electric current ionizes this gas and creates a self-contained plasma ring (the "CT"). Then a fast current pulse compresses and accelerates the CT by electromagnetic forces. This CT is then injected into the tokamak plasma.

Experiments on the CT fueling of small tokamaks have been carried out on TdeV [3-6], JFT-2M [7-9], TEXT [10] and STOR-M [11]. There is sufficient evidence in these experiments to show that CTs can penetrate magnetic fields and non-disruptively fuel tokamak discharges. Experiments on the injection of

corresponding author's e-mail: raman@mailhost.aa.washington.edu
**permanent affiliation: University of Washington, Seattle, WA, USA*

CTs into a larger plasma cross-section are needed to develop this concept for reactor applications. CT injection experiments are under consideration for the Large Helical Device [12]. 3D MHD simulations of the interaction of the CT with a target magnetized plasma are under development at the National Institute for Fusion Science [13].

Experimental demonstration of the formation of milligram (mg) compact toroids on the Marauder device [14] and acceleration to reactor relevant velocities [14-17] means that no extrapolation from small devices is needed for the design of a large tokamak CT fueler.

This paper is organized as follows. In Sec. **2** we describe the basis for the physics model, Sec. **3** describes the injector layout. The next section describes the design for a novel passive superconductor shield. Following this, issues related to electrode erosion are discussed. Section **6** describes the pulsed power system. The final section is a brief summary of this paper.

2. Physics Basis

Early theoretical work by Perkins *et al.* and Parks [1,2] studied the penetration, slowing down and reconnection processes of a CT penetrating a tokamak plasma. A primary condition in these models is that the CT should have sufficient kinetic energy density ($\rho V^2/2$) to exceed the target magnetic field energy density ($B^2/2\mu_o$) so that the target magnetic field lines could be pushed aside during CT penetration. There are other aspects of the models that describe the slowing down of the CT due to the toroidal field gradient, Alfvén drag and tilting of the CT due to alignment of the dipole moment of the CT with that of the tokamak. These are yet to be experimentally measured and verified. If the CT mass (i.e., total fueling particles per CT) is fixed, these effects which act to reduce the CT velocity (i.e., magnetic force from the toroidal magnetic field gradient and Alfvén drag force) can be reduced by increasing the CT plasma density. With higher density, the CT size can be reduced and there is less CT cross-sectional area, and therefore less retarding force from the toroidal field gradient. The Alfvén drag force, which is proportional to the velocity [2], will also become smaller at higher CT plasma density. In order to meet the primary condition ($\rho V^2/2 = B^2/2\mu_o$), a CT with higher plasma density requires less velocity. Since the power to accelerate the CT scales as the kinetic energy of the CT ($KE = MV^2/2$), increasing the CT plasma density reduces power consumption of the CT fueler due to the reduced forces and velocity to penetrate a tokamak plasma.

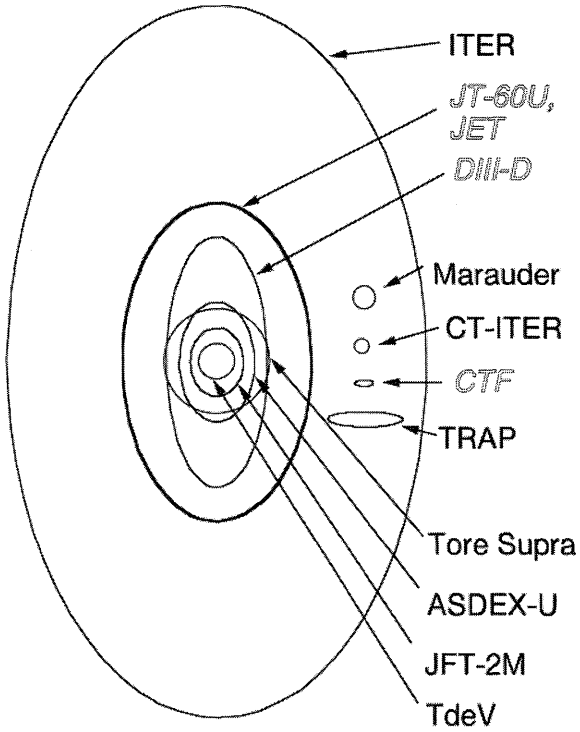

Fig. 1 Relative minor cross-sections of various tokamak plasmas and of compact toroid plasmoids. Note that injection of CTF sized CTs into DIII-D or JT-60U sized plasmas will result in localized fueling at reduced level of perturbation to the target tokamak.

The basic penetration model used is that the kinetic energy density of the CT should exceed the target magnetic field energy density by a factor of 2. This increased energy density requirement is to provide greater flexibility on the part of the injector. In Fig. 1, we show the relative minor cross-sections for various tokamak plasmas and of CT plasmoids. For a localization parameter defined as L_{CT}/a, where L_{CT} is the length of the CT and 'a' is the tokamak minor cross-section, this figure shows that present experiments (for example CTF on TdeV) cannot do localized fueling and in addition these CTs will perturb the tokamak to a much greater extent than injection of similar sized CTs into a larger cross-section plasma. Near term experiments on devices such as DIII-D and JT-60U, should provide sufficient data for the validation of the design for high field tokamak experiments and reactors.

3. Injector Layout

The primary injector parameters for the JT-60U CT

fueler are provided in Table 1. Figure 2 shows a schematic diagram of the conceptual CT fueler for JT-60U and the injector layout in relation to the JT-60U Toroidal Field (TF) coil and vacuum vessel. The design is based on the Marauder configuration [14] and the injector dimensions are based on interpolation between the CTF [3] and Marauder devices. The injector Formation and Acceleration regions are 2 m long, with a maximum diameter of 50 cm. This is about 1.7 times larger than CTF-2 and half the size of Marauder.

The injector will consist of a primary high-cost portion that contains the gas valves, insulators, solenoids, heating/cooling systems and power transmission lines. This portion known as the Formation Injector will be common to two different accelerator designs. The formation injector will house both the outer and inner formation electrodes and will become a single assembly. To this will be attached the outer accelerator electrode. The final portion of the injector will be the inner accelerator electrode assembly. This is replaceable, primarily to test two different accelerator configurations.

Table 1 JT-60U CT injector parameters.

CT radius (m)	0.1
CT length (m)	0.2
CT density ($D.m^{-3}$)	3×10^{22}
CT mass (mg)	0.4
$N_{CT}/ N_{JT\text{-}60U}$ (at $<n_e> 3 \times 10^{19}$)	6%
Fueling rate (D/pulse)	1.2×10^{20}
Fueling frequency (Hz)	up to 10
CT injection speed (km/s)	300
CT kinetic energy (kJ)	18
Fraction of gas trapped in CT (%)	–50
Fraction of gas leaked to tokamak (%)	–50
Formation section r/L (m)	0.25 / 0.5
Accelerator section r/L (m)	0.25 → 0.1 / 1
Total CT injector length (m)	2

The reference accelerator configuration is the self-similar geometry proposed as the final version of the Marauder device [14] but never built and experimentally tested. In this configuration, the accelerator mean radius to electrode gap remains constant throughout the acceleration process. In the second version, the accelerator gap radius remains the same throughout the acceleration process. The actual electrode configuration used on the Marauder experiments was in-between these configurations, but closer in shape to the self-similar geometry. Installation of the constant gap electrode simply involves pulling the inner injector assembly out axially from behind the injector and replacing the front accelerator section.

During acceleration, the CT will undergo self-similar compression. During such compression, the CT length decreases in proportion to its radius while the CT magnetic fields increase inversely in proportion to the

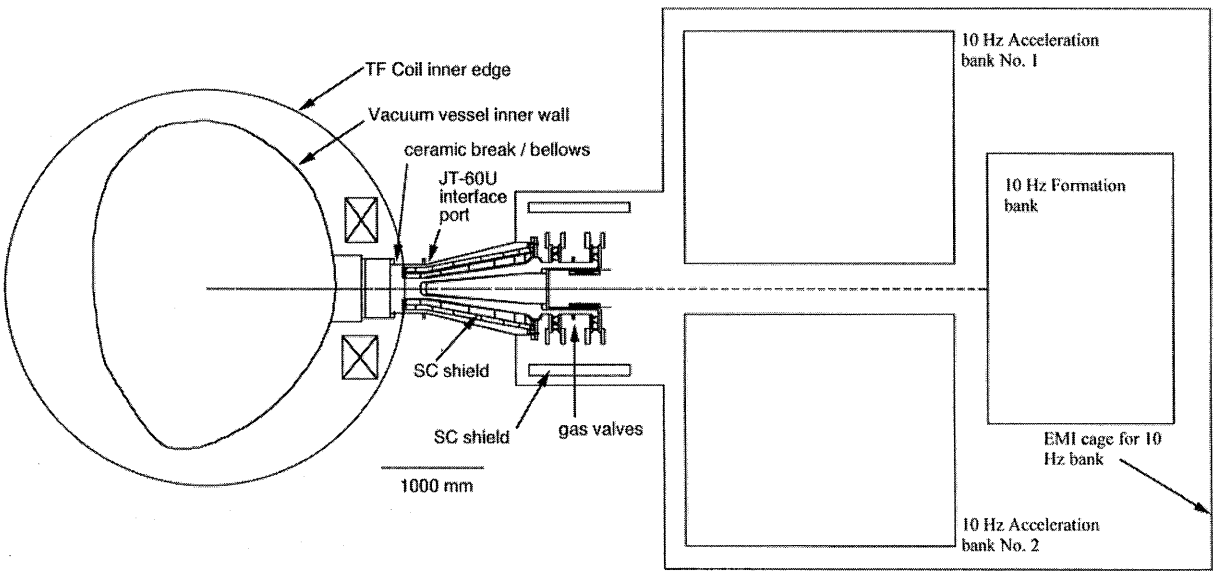

Fig. 2 Schematic of CT injector layout for JT-60U.

decrease in CT volume [17]. The compression length is chosen to be sufficiently long so as not to generate shock waves during compression. As the CT size is reduced due to compression, the increasing CT magnetic field can be made to compensate for the decreasing magnetic field due to decay. In this design, because of the short injector length, the absolute value of the magnetic field will increase as the CT is compressed. Compression will also cause the CT beta to increase some, but the final beta will be less than 10%.

30 fast pulse gas valves will be used to inject the gas needed for CT formation. These will be placed azimuthally around the injector outer formation electrode at the axial location shown in Fig. 2. The specific valve used for this purpose will be the fast pulse gas valve manufactured by the General Valve Corporation, a subsidiary of Parker Hannifin, New Jersey, USA. Ten such valves were purchased for the CTF-2 injector and experimentally tested on a test stand to determine if they are capable of injecting sufficient amounts of gas at short gas pulse widths and with high valve reliability. Experiments on the test stand were successful, and future operations with the CTF-2 injector will use these valves. These valves produce reproducible gas pulses and inject sufficient amount of gas for the generation of 0.4 mg CTs for the JT-60U injector.

CTs will not use all the fuel gas injected into the formation region. Present CTs (except the Marauder device) trap around 10–20% of the injected gas, largely because present gas valves are not fast enough to supply large amounts of gas on short pulses. In addition, reliable start of ionization requires a peak gas pressure of –200 mTorr at the < 9 kV formation voltages presently used. For the JT-60U injector, the operating voltage for the formation gun will be 30–36 kV. For Marauder, at 70 kV, the gas trapping fraction is about 70–90%. We expect a trapping fraction in the ≥ 50% range for this injector. The balance 50% of the unused gas will flow into the tokamak chamber and contribute to edge fueling. The injection of 0.4 mg CTs at 10 Hz corresponds to a deep fueling rate of 2.3 $Pa \cdot m^3/s$; this is similar in magnitude to the fueling from gas injection fueling for steady state sustainment of JT-60U discharges. For demonstration of deep fuelled CT discharges at low densities, He glow discharge cleaning would be necessary to reduce the fueling contribution from the walls and to use the wall as an additional pumping medium. For fueling discharges at higher tokamak densities ($\sim 10^{20}$ m^{-3}), no specific wall conditioning would be necessary.

High throughput turbo or cryo pumps are not included in this design to pump out left over gas from the CT formation phase as experience with the CTF and CTF2 injectors has shown such schemes to be ineffective in pumping out the unused gas. Therefore, a higher voltage operation for the formation injector is used to increase the gas coupling fraction to the CT. A fueling system for reactors will require the leaked gas fraction to be even smaller, but as shown by the Marauder device, the fraction of gas trapped by the CT can be increased to the required levels by operating the formation injector at higher voltages.

All plasma facing components will be coated with dense tungsten (100–200 μm) as was used on the CTF devices and more recently for the coating of the inner electrode on the HIT-CTI device in use on JFT-2M. The bias solenoid will be mounted inside the inner formation electrode. This will be electrically isolated from the inner formation electrode with sufficient layers of insulation. The power supplies needed for the injector CT formation and acceleration stages will be placed near the injector to reduce overall external system inductance since this increases the overall system efficiency defined as the fraction of capacitor bank energy that translates to directed CT kinetic energy. The details of the power system are provided in Sec. **6**.

4. Magnetic Shielding

The CT acceleration process involves magnetic forces which act on the CT. Consequently, stray magnetic fields that interfere with the accelerating magnetic fields can impede efficient acceleration. In order that CT penetration into JT-60U be maximized, it is necessary that the CT injector be installed as close as possible to the JT-60U edge plasma. Since CT fueling is a relatively new technology still under development, the success of initial large scale tokamak experiments can be increased by minimizing the CT free-flight distance.

On JT-60U, the maximum fringe fields are due to ripple fields produced by the TF coils, generally referred to as "Toroidal field ripple" in JT-60U literature. For 2 T discharges, at a major radius of 5.3 m, the corresponding fringe TF field is 1 T. At R = 7 m, which corresponds to the beginning of the acceleration region the TF field is 0.1 T. The leading edge of the injector will be positioned at R = 5.3 m. So, magnetic shielding will be required to reduce the fields in the accelerator to the 0.01 T level. The front end of the injector will be aligned with the inner edge of the TF coils.

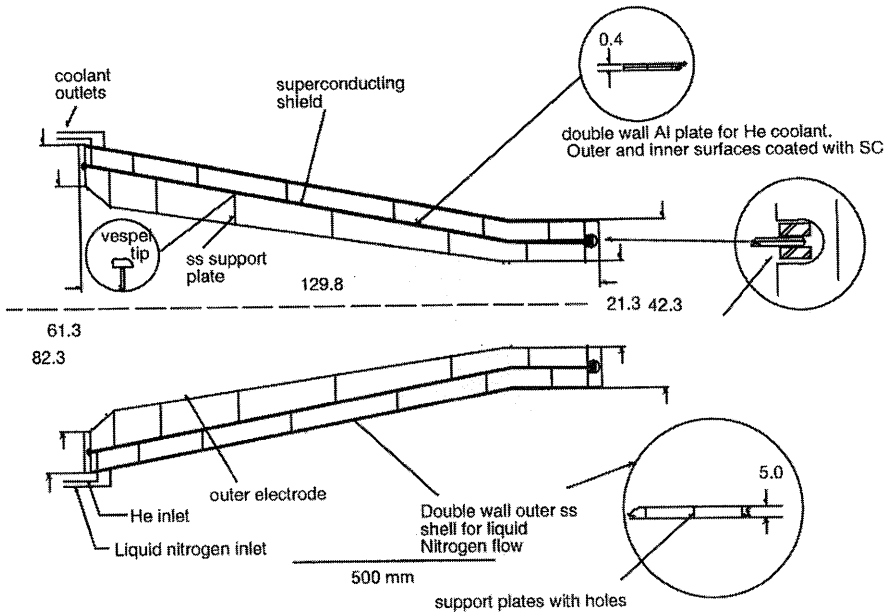

Fig. 3 Reference design for the superconducting shield for the JT-60U CT injector.

At the 1 T level, passive ferromagnetic shields are not suited for this application. For diameters ≥ 20 cm it is impractical to shield fields above 0.5 T as the physical shield dimensions become very large. In addition, future tokamaks/stellarators may operate at even higher fields and efficient fueling of these devices by CTs will require the technology to shield higher levels of magnetic fields. Therefore, a passive super conductor shield will be used.

There is steady progress being made in the field of magnetic shielding using passive superconductors. The need for such shields exist in particle accelerator environments [18] Magnetic Resonance Imaging (MRI) environments [19] where the limit is about 10 gauss for patients with cardiac pacemakers. A passive superconductor has been found to be effective because it lightens the system compared to a ferromagnetic shield, and can shield fields above 2 T which is the saturation level for the best ferromagnetic shields. Sufficient technology exists at present for the design of a superconducting shield for a CT injector for JT-60U and the technology is expected to get easier as new developments continue to be made.

A novel passive super conductor shield design is proposed. For the reference design, a conical superconducting shield is fabricated that closely fits the outside of the accelerator outer electrode. The chosen superconducting material is a NbTi/Nb/Cu multilayer composite as described in reference [20]. Smaller shields using this design have been tested in magnetic fields of up to 0.7 T [21,22] and shields based on other designs have been used to exclude 2 T fields [23,24]. The fabrication techniques are well developed on a small scale [20], and no unusual technology developments are needed. However, a 20% scale model prototype should be tested to fully develop the shield fabrication technology for larger sizes. The shield, shown in Fig. 3, will operate at 4–10 K by use of a He gas flow cooling system, a technology that is now in common use for cooling superconductors to this level.

Reference Design A: In the proposed design, shown in Fig. 3, a 4 mm thick double wall Aluminum plate is fabricated in the form of a cone. This forms the base structure for the SC shield and the medium that will be cryogenically cooled by He gas coolant. On top of this alternating layers of the superconductor, Nb and copper are deposited by a plasma spray process. Based on the work of Sasaki [21,22], the thickness would be –9 μm for NbTi, followed by a thin layer of Nb (–0.5 μm), then the copper substrate also –9 μm. 120 NbTi layers would be used for a total thickness of the layered structure of 1.5 mm. On top of this a reflective layer of gold would be electroplated as a protective layer and to reduce the heat absorption from the outside structure. This assembly would then undergo suitable heat treatment process at about 350°C [21,22]. Higher

levels of heat treatment did not improve performance and use of a lower temperature process allows the use of Aluminum as the base structure as it is a third the weight of copper with nearly as good thermal conductivity.

Shielding capability of multilayer superconductors is achieved due to pinning at superconductor/non-superconductor (S/N) interfaces. In the fabrication of NbTi wires, for example, flux pinning centers are introduced by metallurgical means for increasing the critical current density. Small particles of α-Ti are precipitated by heat treatment and these particles are then changed to thin, long ribbons by drawing. In a layered SC, the α-Ti precipitations are formed during the procedure used to heat treat the sample. The specific heat treatment method determines the level of critical current density a layered SC can attain and its shielding capability. Since the heat treatment process is important in determining the final critical current performance of the superconductor, should a higher temperature process found to be necessary, based on the prototype experiment, then the Aluminum would be replaced by Copper.

Design B: An alternate fabrication process is to wind 0.5 mm diameter Nb-Ti-Ta-Zr superconductors in an oblique 45 degree winding as in the reference of Takahata [24]. A total of 4 windings with adjacent windings having opposite winding polarity, should be capable of shielding more than 2 T fields as demonstrated by this reference. This would then be impregnated in a matrix of Indium as this is superior to Wood's metal [23]. The total superconductor plus substrate thickness would be about 2 mm, similar to the thickness of the Reference design A. This design has the advantage that (a) the shielding parameters have been adequately demonstrated for the type of field orientations expected on JT-60U, (b) the superconductor is stable to flux jumps up to 3.4 T providing a much higher safety factor and (c) pre-fabricated superconducting wire can be purchased so that there is no development cost for the superconductor and (d) the winding techniques are conventional and can be carried out by lower cost machine shops.

The outer shells of the shield will be cooled by liquid nitrogen circulating in a double wall stainless-steel shell. The region between the outer double shells that contain liquid N_2 coolant and the SC structure will be evacuated to moderate vacuum to reduce conduction heating. This would lower the surface temperature of the outer shell to about 77 K from the otherwise –600 K as the JT-60U vacuum vessel is heated to –300°C. The requirements on the He cryogenic system would then be much less demanding. The radiative heating is then < 20 Watts. Small thin tubular legs will be dispersed in the annulus to support the SC structure. The region between the inner shell and the injector outer electrode will contain 0.5 cm thick vacuum compatible insulating material for thermal and electrical insulation.

5. Impurity Control

Since CTs are in contact with metal walls during their formation and acceleration stages, sputtering and arcing can release atoms which contaminate the CT. The primary impurities are carbon and oxygen trapped in the walls, and metals from erosion of the electrodes.

In the JT-60U CT fueler, carbon and oxygen are reduced by baking the electrodes and by repetitively pulsing the fueler prior to (and during) operation in order to condition the surfaces. Steel impurities are eliminated by coating the electrodes with tungsten. Previous CT work in Japan [25] and on RACE concluded that high-Z impurities were not efficiently trapped by the high velocity CT. And recent work with the CTF fueler on TdeV [6] concluded that the W addition to the tokamak plasma from CT injection was less than 2×10^{-5} W atoms/electron in the tokamak plasma.

A design aspect in which this injector is different from CTF/RACE is that copper will not be used as a vacuum boundary. The reason is to eliminate o-rings as vacuum interfaces. All vacuum boundary seals will be made with conflat gaskets. This should allow baking the injector to about 300°C at which temperature, gaseous impurities should not pose problems. At 300°C, the resistivity of copper is 3.8×10^{-8} Ωm and that of W is 13.23×10^{-8} Ωm. For a 20 μs formation discharge, the skin depth in copper is 0.44 mm while that in W is 0.82 mm; for SS-304 it is about 28 mm. Thus SS alone will not be a suitable conductive shell. The procedure to fabricate the electrode is to initially start with a stainless vacuum boundary that is welded to suitable conflat flanges. After suitable heat treatment and annealing, the plasma facing surface would be electroplated with a 0.5 mm thick layer of pure copper, which is based on the residence time of the CT at any given location in the accelerator. A suitable thickness of W would then be deposited on this copper surface by the vacuum plasma spray process. A 100 μm layer of W for the outer electrodes and a 200 μm layer for the inner electrodes should be sufficient. The tips of the inner electrode will be subjected to greater erosion, so the leading 10 cm of

this electrode will be coated with a thicker layer (500 μm) of W. 100 μm thick coatings of W with very low porosity (< 2%) have been demonstrated on the CTF-2 injector. Higher thickness coatings have recently been applied to the HIT-CTI injector's inner electrode now in operation on the JFT-2M tokamak at the Japan Atomic Energy Research Institute.

For cold cathodes, the erosion rate of W is 0.62×10^{-7} kg/C [26]. The total charge transfer for the formation gun is about 6–10 C resulting in an erosion of 0.6×10^{-6} kg of W per shot. Most of this will occur along a 10 cm length at the flux foot-print location. For the formation inner electrode this translates to an erosion of 0.2 nm per shot. For a 200 μm W thickness of the cathode, this should result in a lifetime of 10 years based on a 10 second pulse and 40 shots per day and 25 days per year of CT injector related experiments. The total effective charge transfer for the accelerator will be about the same leading to similar total mass erosion rates. However, the lifetime will be much longer than 10 years as the current sheath translates over the entire length of the accelerator thereby spreading the erosion uniformly over the entire length.

At present, there is no evidence for entrainment of the eroded metals in the CT. Recent tokamak injection experiments on TdeV and JFT-2M have not shown evidence for contamination of the tokamak discharge by metallic impurities. A 5 eV W ion travels just 1.5 cm during a typical 10 μs formation discharge, while the CT formation region is > 10 cm from the region of formation discharge initiation, which seems to explain the poor coupling of W to the CT. However, the eroded impurities will, over time, collect on the electrode surface. The injector annulus would be flushed with high-pressure gas at required intervals to remove the eroded deposits.

6. Power Supplies

The power supplies for the JT-60U injector will use capacitors for energy storage and recent design spark gaps for switching. The Maxwell Technologies group conducted a capacitor design study as a result of a request by the Canadian Fusion Fuels Technology Project. This study resulted in the design of a new (next generation) power capacitor that can be operated at up to 20 Hz. The estimated life is 3×10^7 full power pulses at 20 Hz. New generation spark gaps have the primary advantages of long life, low cost and capability to operate at 10 Hz. Recent developments in this area were motivated by the need to find replacements for ignitrons which contain mercury as the switching medium. The switch model SW-50K manufactured by Maxwell Technologies would meet the requirements for the JT-60U injector. This switch has a rated life of about 12,000 shots before electrode replacement. The electrode replacement cost is low and they would be replaced at periodic intervals. For future injectors operating on a long duty cycle (1,000s of seconds), switches such as the new generation High Current Thyristors would be better suited [27,28]. But, these are expensive and the technology involved in incorporating these to high voltage pulsed power systems is more difficult. For JT-60U experiments, the model SW-50K spark gap switches are adequate. The engineering parameters based on the above capacitor and spark gap are provided in Table 2. The circuit equations were solved using the SPICE circuit simulation code. The resulting output is shown in Fig. 4.

Injector operation at 10 Hz involves the charging and discharging of the capacitor banks associated with

Table 2 Power supply parameters.

Parameter	Acceleration Bank	Formation Bank
Capacitance (μF)	200	160
Maximum Voltage (kV)	36	36
$R_{capacitor}$ (mΩ)	0.1	0.13
$L_{capacitor}$ (nH)	0.5	0.63
Rsafety (mΩ)	5.0	6.25
$L_{resistor}$ (nH)	0.2	0.252
L_{switch} (nH)	1.68	2.1
R_{cable} (mΩ)	0.38	0.47
$L_{transmission\ cable}$ (nH)	25.2	31.5
R_{load} (mΩ)	5	5
L_{load} (nH)	15.98	40.58
$I_{maximum}$ (kA)	1000	700
Maximum stored energy (kJ)	130	98
No. of modules	100	80
No. of capacitors / module	1	1
No. of RG-218U cables / module	2	2
Length of RG-218U cables (m)	20	20
Physical arrangement: No. of units	2	1
Floor foot-print: No. caps per row	10	10
No. of rows	5	8
Foot print (m^2)	9.4×2	15.8
Height (m)	2	2
Weight (kg) [aux. = 15% cap wt.]	$5,577 \times 2$	8,900
Volume (m^3)	19×2	32
Overall resistance (mΩ)	10.48	11.85
Overall inductance (nH)	43.56	75.06
Bank quarter cycle time (μs)	4	5
Peak current at 36 kV (MA)	1.5	1.2

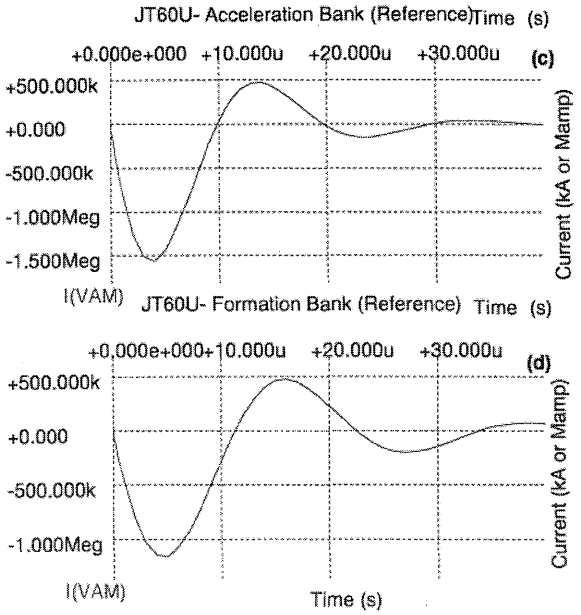

Fig. 4 Circuit currents from simulation using the Spice circuit simulation code for the Acceleration and Formation stages.

the gas valves, the bias solenoid, the CT formation bank and the CT acceleration bank 10 times every second. This is similar to the operation of pulsed power systems envisioned for the laser inertial fusion program except that the power supplies associated with the CT injector are much smaller in size. In the formation bank all of the sub-modules will be switched at the same time. The modules in the accelerator bank will all be switched at the same time after providing the CT some time (about 25 μs) to relax and to form an axially symmetric structure in the formation chamber. The reason for the large number of modules (instead of a single large assembly) is to reduce the development, fabrication and maintenance cost.

Power supply layout: The formation capacitor bank will be composed of 80 individual modules and the accelerator bank will contain 100 such modules. The use of a standard module for both systems will reduce the development cost since only a few modules need to be built and tested.

The formation bank will be placed directly behind the injector. The actual foot-print of the capacitors measures 2.7 m wide × 3.7 m long. The acceleration capacitor bank will consist of two units each housing 50 capacitor modules. Each of these units will be placed on either side of and behind the injector. The capacitor floor space occupied by each bank measures 2.9 m × 2.7 m. Figure 2 shows the location of these banks in relation to the injector.

The CT injector will generate EMI noise that can interfere with tokamak diagnostics. Two methods will be used to minimize and to shield this noise from other systems. The first scheme involves impedance matching cable terminating resistors. The electrical power feed cables used for connections between the capacitor banks and the injector will be RG-218 coaxial cables with an impedance of 50 Ω. At the junction to the injector, these cables will be terminated with 50 Ω resistors to minimize reflections in the cable. The second scheme involves housing all the power supplies and the bulk of the back portion of the injector in an EMI cage. The cage will be fabricated out of thin Aluminum or Copper sheets with fiberglass corner beams for structural support. It will be sufficiently large in size so as to allow maintenance work to be performed inside the cage. A 15 kW-hour air-conditioning unit would be used to cool the EMI cage. The ambient temperature inside the room would be maintained below 10°C, to allow internal resistors to dissipate heat during the 15 minute interval between experiments. The calculated floor space area is accurate to within 15%.

7. Summary

A design description of a Compact Toroid injection system for the JT-60U tokamak is provided. This fueling system would inject 2.3 Pa·m^3/s of deuterium fuel in the form of high velocity magnetized plasmoids. The injected CTs would deep fuel the discharge thereby possibly contributing to improved plasma performance. Design descriptions have been provided for the fabrication of a novel passive superconducting shield to exclude the 1 T magnetic fields in the vicinity of the CT injector. Design details for a 10 Hz pulsed power system to meet the needs of this fueler are provided. Extrapolation from this design to a reactor CT fueler would primarily require the fabrication of a pulsed power system based on Thyristor switching.

Acknowledgments

We would like to thank Dr. T. Ando of JAERI for educating us on the current state of superconductor technology for passive applications. Thanks to Dr. P. Gierszewski of CFFTP for initiating the Canadian CT effort and for first noting the advantages of high temperature electrodes for CT injector applications. Special thanks to Drs. M. Nagami and R. Yoshino for

their support of this work. Early experimental efforts by J.H. Hammer and C.W. Hartman at LLNL and the theoretical work of L.J. Perkins *et al.*, and P.B. Parks were instrumental in helping to develop the CT fueling concept.

References

[1] L.J. Perkins, S.K. Ho and J.H. Hammer, Nucl. Fusion **28**, 1365 (1988).
[2] P.B. Parks, Phys. Rev. Lett. **61**, 1364 (1988).
[3] R. Raman *et al.*, Fusion Technol. **24**, 239 (1993).
[4] R. Raman *et al.*, Phys. Rev. Lett. **73**, 3101 (1994).
[5] R. Raman *et al.*, *Proc. 24th EPS Conf. on Controlled Fusion and Plasma Physics*, Berchtesgaden, Germany (1997) p.293.
[6] R. Raman *et al.*, Nucl. Fusion **37**, 967 (1997).
[7] T. Ogawa *et al.*, *Proc. 17th IAEA Fusion Energy Conf.*, IAEA-F1-CN-69/EXP1/16 Yokohama, Japan (1998).
[8] H. Ogawa *et al.*, J. Nucl. Mater. **266–269**, 623 (1999).
[9] T. Ogawa *et al.*, Nucl. Fusion **39**, 1911 (1999).
[10] J. Yee and P.M. Bellan, Nucl. Fusion **38**, 711 (1998).
[11] C. Xiao *et al.*, *Proc. 17th IAEA Fusion Energy Conf.*, IAEA-F1-CN-69/EXP3/02 Yokohama, Japan (1998).
[12] J. Miyazawa *et al.*, Jpn. J. Appl. Phys. **37**, 6620 (1998).
[13] Y. Suzuki *et al.*, Nucl. Fusion **40**, 277 (2000).
[14] J.H. Degnan *et al.*, Phys. Fluids B **5**, 2938 (1993).
[15] C.W. Hartman and J.H. Hammer, Phys. Rev. Lett. **48**, 929 (1982).
[16] J.H. Hammer, C.W. Hartman and J.L. Eddleman, Phys. Rev. Lett. **61**, 2843 (1988).
[17] A.W. Molvik *et al.*, Phys. Rev. Lett. **66**, 165 (1991).
[18] B.C. Brown, IEEE Trans. Mag. **27**, 1985 (1991).
[19] W. Pavelic *et al.*, Radiology **147**, 149 (1983).
[20] I. Itoh and T. Sasaki, Cryogenics **35**, 403 (1995).
[21] T. Sasaki and I. Itoh, Cryogenics **36**, 497 (1996).
[22] T. Sasaki and I. Itoh, Cryogenics **35**, 335 (1995).
[23] K. Seo *et al.*, Cryogenics **31**, 524 (1991).
[24] K. Takahata *et al.*, IEEE Trans. Mag. **25**, 1889 (1989).
[25] T. Uyama *et al.*, Nucl. Fusion **27**, 799 (1987).
[26] J. Wesson, *Tokamaks* (Clarendon Press, Oxford, 1987) p.217.
[27] P. Gierszewski, R. Raman and D. Hwang, Fusion Technol. **28**, 619 (1995).
[28] R. Raman and P. Gierszewski, Fusion Eng. Des. **39–40**, 977 (1998).